Supporting Information

Sacrificial Cobalt-carbon Bond Homolysis in Coenzyme B_{12} as a Cofactor Conservation Strategy

Gregory C. Campanello[1], Markus Ruetz[1], Greg J. Dodge[1,2], Harsha Gouda[3], Aditi Gupta[1], Umar T. Twahir[4], Michelle M. Killian[5], David Watkins[6], David S. Rosenblatt[6], Thomas C. Brunold[5], Kurt Warncke[4], Janet L. Smith[1,2], and Ruma Banerjee[1*]

[1]Department of Biological Chemistry, University of Michigan, Ann Arbor, MI 48109-0600

[2]Life Sciences Institute, University of Michigan, Ann Arbor, MI 48109-0600

[3]Indian Institute of Science Education and Research, Pune, India 411008

[4]Department of Physics, Emory University, Atlanta, GA 30322-2430

[5]Department of Chemistry, University of Wisconsin, Madison, WI 53706

[6]Department of Human Genetics, McGill University, Montreal, QC H3A 1B1, Canada

*Address correspondence to: Ruma Banerjee, Tel: (734) 615-5238; E-mail: rbanerje@umich.edu

Materials and Methods

Materials. All primers used in this study were purchased from Integrated DNA Technologies. Most reagents including PPP_i, D_2O, ATP, and AdoCbl were purchased from Sigma-Aldrich. Methanol and acetonitrile were from Fisher Scientific and [U-^{13}C]-ATP was from Cambridge Isotopes.

Cloning, expression, and purification of human ATR proteins. An expression clone of human ATR (generously provided by Thomas Bobik, Iowa State University) was used as a template to amplify the cDNA using the following primers with NdeI (forward): 5'-AAAA**CATATG**CCTCAGGGCGTGGAAGACGGG-3' and XhoI (reverse) 5'-AAAAAA**CTCGAG**T CAGAGTCCCTCAGACTCGGCCG-3' restriction sites. The PCR product was cloned into a pET-28b vector and the resulting recombinant protein contained a thrombin-cleavable, N-terminal His-tag. BL21(DE3) *E. coli* was transformed with the expression construct and a single transformant was inoculated into 100 ml of Luria Bertani (LB) medium containing 50 µg/ml kanamycin and grown overnight at 37 °C. This culture was used to inoculate 6 liters of LB medium and grown to an OD_{600nm} of 0.6. Protein expression was induced with 0.5 mM IPTG and cells were grown overnight at 20 °C, and harvested by centrifugation. The cell pellet was resuspended in ATR lysis buffer (50 mM Tris, pH 8.0, containing 300 mM NaCl, 10 mM imidazole, 1 mM TCEP). Following cell lysis by sonication, the supernatant was loaded onto a 25 ml Ni(II)-NTA column and ATR was eluted using 200 ml of a linear gradient (10-200 mM imidazole in the same buffer). The N-terminal His tag was cleaved using thrombin (500 U, Pfizer), overnight at 4 ˚C and passed through a 5 ml Benzamidine column (GE life Sciences) to remove thrombin. Finally, ATR was dialyzed against 50 mM HEPES buffer, pH 7.5, containing 150 mM KCl, 2 mM $MgCl_2$, 2 mM TCEP, 5% glycerol.

For X-ray crystallography, an N-terminal Δ18 ATR variant was generated by mutagenesis using the following forward primer: 5'-CGCGGCAGCCATATGCCCAAGATTTACACC -3'. The second primer had the reverse sequence. The truncated ΔN18 ATR was purified in the same manner as

the full-length protein and exchanged into 20 mM HEPES buffer, pH 7.5 containing 100 mM NaCl, 1 mM DTT, 2 mM and $MgCl_2$ after purification. R186Q ATR was generated using the following forward primer: 5'-TGCATTTCTGCCAGGCCGTGTG-3' and a reverse primer with the complementary sequence. The R186Q ATR mutant was purified like the wild-type protein.

Cloning, expression and purification of human MCM. A synthetic gene for human MCM that was codon optimized for *E. coli* expression was obtained from Genscript and cloned into the pET28b vector using the Nco I and Xho I restriction sites. The construct contained a C-terminal TEV-cleavable His-tag. Recombinant human MCM was expressed in terrific broth as described previously[1] with the exception that 3% DMSO was added to improve protein solubility. After harvesting, cells were resuspended in 50 mM Tris-HCl, pH 8.0, containing 500 mM NaCl, 20 mM imidazole and 5% glycerol and lysed by sonication. The supernatant was loaded onto a 25 ml Ni(II)-NTA column and eluted using 250 ml of a linear gradient ranging from 20-200 mM imidazole in the same buffer. Next, the C-terminal His tag was cleaved using His-tagged TEV protease (1:50 (m/m) TEV:MCM) overnight at 4 °C. The next day, TEV was added again and cleavage was continued under the same conditions. TEV was removed by passing through a Ni(II)-NTA column and the flow-through was collected. The cleaved protein was then loaded onto a Source Q column (Omnifit) equilibrated with 50 mM HEPES, pH 7.3, 25 mM NaCl, 5% glycerol. MCM was eluted with a linear gradient of 25-500 mM NaCl in the same buffer. Purified MCM was dialyzed against 50 mM HEPES pH 7.5, 150 mM KCl, 2 mM $MgCl_2$, 2 mM TCEP and 5% glycerol before use.

Buffer conditions for experiments. Unless noted otherwise, all titrations and kinetic experiments were performed in Buffer A containing 50 mM HEPES pH 7.5, 150 mM KCl, 2 mM $MgCl_2$, 2 mM TCEP and 5% glycerol.

Electronic absorption spectroscopy to measure formation of the PPPi•AdoCbl•ATR ternary complex. AdoCbl was loaded onto ATR by mixing 60 μM AdoCbl with 60 μM ATR (trimer) in Buffer A under anaerobic conditions. Addition of PPP_i led to formation of intermediate

X and the dependence of ΔA389 nm on the concentration of PPP_i was plotted to generate binding isotherms. The data were fit to a single PPP_i binding per active site containing AdoCbl using Dynafit.[2] Similarly, wild-type and R186Q ATR were titrated into 30 μM AdoCbl in the presence of either 1 mM (wild-type) or 5 mM (mutant) PPPi to monitor the formation of intermediate X. The titration was performed in triplicate at room temperature.

Assays for monitoring AdoCbl transfer between ATR and MCM. To monitor AdoCbl transfer from ATR to MCM, ATR (20 μM trimer) was mixed with 20 μM AdoCbl and the absorbance spectrum was recorded. Next, MCM (20 μM dimer) was added and the spectra were recorded every 2-5 min for a total of 60 min at room temperature. The kinetics of ATP-driven AdoCbl transfer following in situ AdoCbl synthesis was monitored by forming 20 μM cob(I)alamin under anaerobic conditions using titanium citrate (80 μM), followed by addition of ATR (20 μM) to the cuvette at 20 ˚C. AdoCbl synthesis was initiated by addition of 1 mM ATP, and its transfer to MCM (20 μM) added simultaneously to the reaction mixture, was monitored. The change in absorbance at 530 nm corresponding to base-on AdoCbl was recorded as a measure of cofactor transfer from ATR to MCM. The k_{obs} for transfer was estimated from the initial reaction velocity for base-on AdoCbl formation. The concentration of AdoCbl transferred was determined using $\Delta\varepsilon_{530\ nm}$ of 6.9 cm^{-1} mM^{-1} [$\varepsilon_{530\ nm}$(AdoCbl•MCM)–$\varepsilon_{530\ nm}$ (intermediate X)). The experiment was performed in triplicate. To assess AdoCbl transfer in the reverse direction (i.e. MCM to ATR), MCM (20 μM dimer) was loaded with AdoCbl (20 μM) and the absorption spectrum was recorded. Addition of ATR (133 μM trimer) elicited no significant spectral changes even after 20 min.

Rate of PPP_i driven Co–C bond homolysis. The rate of Co-C bond homolysis was determined in the presence of ATR (20 μM trimer) and AdoCbl (20 μM) to which PPP_i (1 mM) was added at room temperature. Spectra were recorded every minute. To determine the kinetics of O_2-driven Co–C bond homolysis, the experiment was repeated at 20 °C and the change in absorbance at 465 nm (corresponding to 4-coordinate cob(II)alamin formation) was monitored. The k_{obs} was

calculated as described above except that a value of $\Delta\varepsilon_{465\ nm}$= 8.0 cm^{-1} mM^{-1} for [ε_{465nm} (4-cob(II)alamin•ATR) – ε_{465nm}(intermediate X)] was used. The experiment was conducted in duplicate.

Effect of PPPi R186Q ATR•AdoCbl. Given its weak affinity for AdoCbl, formation of intermediate X on R186Q (333 μM) was monitored by reconstituting it with 53 μM AdoCbl under anaerobic conditions at room temperature. After passing the mixture through a Centricon filter, the absorption spectrum indicated that 58% of the cofactor was bound to R186Q ATR. Next, PPPi (5 mM) was added for 2 min and the absorption spectrum was recorded. The mixture was passed through a 10 kDa MWCO membrane to separate unbound cofactor. Under these conditions, 89% of the cofactor remained bound to R186Q ATR and resembled the spectrum of base-on NpCbl. In Figure 3c, difference spectra (protein bound-unbound cofactor) are shown before and after addition of PPP_i. To monitor PPPi-induced homolysis, the same experiment was performed except under aerobic conditions. Spectra were recorded every 2 min and showed formation of aquocobalamin.

Isothermal titration calorimetry. ITC experiments were performed using a MicroCal VP-ITC with a sample cell volume of 1.8 ml and a 300 μl injection syringe. All experiments were performed at 20 ºC. Samples were filtered through a 0.2 μM filter into degassing tubes, and degassed under vacuum with a ThermoVac sample degasser at 4 °C. For ATP binding to ATR, one 5 μl injection and subsequent 25 x 10 μl injections of 1.2 mM ATP were made to 60 μM ATR with 5 min spacing to allow for equilibration. ITC data were analyzed using ORIGIN 7.0 and fit to a two-site binding model with the N value fixed at 1.0. For binding of AdoCbl to wild-type and R186Q ATR, one 5 μl injection and subsequent 25 x 10 μl injections of AdoCbl (6 mM) were added to R186Q ATR (60 μM) with 7 min spacing between injections. However, no binding of AdoCbl was detected to R186Q ATR.

ATR activity assays. Cob(I)alamin was formed under strictly anaerobic conditions by adding ~10 equivalents of titanium citrate to 32 μM cob(II)alamin. The concentration of cob(I)alamin was estimated using $\varepsilon_{386\ nm}$= 28.0 cm^{-1} mM^{-1} [3]. ATP (1 mM) and wild-type (1 μM trimer) or R186Q (1 μM) ATR were added to initiate AdoCbl synthesis. The AdoCbl concentration was estimated using $\Delta\varepsilon_{522\ nm}$ = 5.04 cm^{-1} mM^{-1} for [$\varepsilon_{522\ nm}$ (free AdoCbl) – $\varepsilon_{522\ nm}$ (cob(I)alamin)]. The specific activity of ATR (expressed as μmoles of AdoCbl formed min^{-1} mg ATR^{-1}) was used to determine the k_{cat} at 25 ˚C.

Synthesis of [U-^{13}C-Ado]-Cbl. ATR from *Cupriavidus metallidurans* [4] was used to synthesize [U-^{13}C-Ado]-Cbl. In a 1 ml reaction volume, 1 mM cob(I)alamin in 100 mM potassium phosphate pH 7.5, was prepared by reducing aquocobalamin with 4 mM titanium citrate. Then, ATR (30 μM) in 250 mM HEPES pH 7.5, containing 100 mM NaCl and 5 mM $MgCl_2$, and [U-^{13}C-Ado]-ATP 1 mM were added to initiate [U-^{13}C-Ado]-Cbl synthesis under strictly anaerobic conditions. After 1 h, the reaction was quenched with 100 μl of 2 M trichloroacetic acid. The reaction mixture was passed through two Sep-Pak C_{18} cartridges (Waters) equilibrated with H_2O and the product was eluted with 3 x 10 ml washes of MeOH. AdoCbl was flash-frozen, lyophilized, and stored at -80 °C as a powder until later use. [U-^{13}C-Ado]-Cbl was assessed by HPLC to be >99% pure.

Synthesis of neopentylcobalamin (NpCbl or Coβ-(2,2-dimethylpropyl)-cobalamin). NpCbl was prepared by a modification of the published procedure [5-6]. The reaction was carried out inside an anaerobic chamber (O_2 <0.3 ppm) and protected from light. In a black 1.5 ml sample tube, 25 mg aquocobalamin•HCl (18.1 μmol) was dissolved in 1 ml methanol containing 50 mg NH_4Br (5% w/v). The solution was then transferred to a second sample tube containing 100 mg zinc dust and shaken at room temperature for 5 min. Then, 5 μl neopentyl iodide (37.7 μmol) was added and the tube was shaken for 3 min. The tube was centrifuged for 3 min at 12,000 × *g* and the supernatant transferred to 10 ml of 1 M HCl. The solution was then applied to a 1 g RP-

C18 cartridge (Waters). The cartridge was washed with 10 ml H_2O, 1 ml 1 M HCl and then, 10 ml H_2O. The product was eluted from the cartridge with 5 ml methanol. The solution was diluted with 2 ml H_2O, flash frozen in liquid N_2 and dried by lyophilization. NpCbl (13.2 mg 48% yield) was obtained as an orange powder and had absorption spectral properties in neutral and acidic pH that were identical to those reported previously [5-6].

The purity of NpCbl was judged to be 90% by analytical HPLC using an RP-18 column (Phenomenex Luna C-18, 4.6 × 250 mm) and the following solvent system: buffer A: 0.1 % TFA in H_2O; buffer B: 0.1 % TFA in acetonitrile; gradient: 0 – 2 min: 2% B isocratic; 2 – 20 min: 2 – 40 % B; 20 - 25 min: 40 – 60 % B; 25 – 30 min: 60% B isocratic; 30 – 33 min: 60 – 2 % B; 33 – 37 min 2 % B isocratic. Under these conditions NpCbl eluted at 21.1 min.

NMR spectroscopy. Samples for NMR analysis contained ATR (300 μM trimer), [U-^{13}C-Ado]-Cbl (750 μM) in 50 mM potassium phosphate pH 7.5, containing 150 mM KCl, 2 mM $MgCl_2$, 2 mM TCEP and 10% D_2O (v/v) to which PPP_i (5 mM final concentration) was added. NMR spectra were recorded before and after addition of PPP_i at 25°C.^{13}C spectra were recorded on a Varian VNMRS 700 spectrometer equipped with Varian 5 mm PFG AutoX broadband probe, operated at 175.97 MHz. Spectra were obtained with an acquisition time of 3 sec per scan and 3000 scans were accumulated. ^{13}C spectra were calibrated by the indirect referencing method [7]. The sensitivity was improved by applying an exponential window function using a line broadening of 30 Hz (- PPP_i) and 10 Hz (+ PPP_i). A 2D ^{1}H-^{13}C HSQC experiment was recorded on the same instrument using the gHSQCAD pulse sequence with 1024 data points in t1 and 128 data points in t2. A bandwidth of 10 ppm for ^{1}H centered around the residual water peak and 220 ppm for ^{13}C was used with 56 scans per t1 increment.

Magnetic circular dichroism spectroscopy. To a solution of ATR containing AdoCbl in 50 mM HEPES pH 7.5, 150 mM KCl, 2 mM $MgCl_2$, 2 mM TCEP and 5% glycerol, PPP_i was added under aerobic conditions Spectral changes corresponding to formation of 4-coordinate

cob(II)alamin bound to ATR were monitored after addition of PPP_i. When no further spectral changes were observed, the final MCD samples were prepared by mixing the above protein solution with 55% (v/v) of the glassing agent glycerol prior to injection into an MCD sample cell and freezing in liquid N_2.[8] The final sample concentration was: ATR (99 μM), AdoCbl (197 μM) and PPP_i (600 μM). Low-temperature (4.5 K) MCD data were collected with a Jasco J-715 spectropolarimeter in conjunction with an Oxford Instruments SM-4000 8 T superconducting magnetocryostat. Contributions from the circular dichroism signal and glass strain were removed from the MCD data by taking the difference between data obtained with the magnetic field aligned parallel and antiparallel to the light propagation axis.

EPR spectroscopy. The X-band EPR measurements were performed on a Bruker ELEXSYS E500 EPR spectrometer using a Bruker ER4123SHQE X-band cavity resonator, and Bruker ER4131VT system for temperature control,[9] Unless specified otherwise, the EPR samples contained: 600 μM wild-type ATR (trimer) and 600 μM cob(II)alamin and 1 mM PPPi or 500 μM R186Q ATR (trimer), 500 μM cob(II)alamin and 5 mM ATP in 50 mM HEPES buffer, pH 7.5, 150 mM KCl, 2 mM $MgCl_2$, 2 mM TCEP and 15% glycerol. Cob(II)alamin bound to wild-type ATR was generated by homolysis of bound AdoCbl (600 μM) in the presence of 1 mm PPPi under aerobic conditions. The following conditions were used to acquire the EPR spectra: microwave frequency, 9.46 GHz; power, 2.0 mW; modulation amplitude, 1.0 mT; modulation frequency, 100 kHz; temperature, 120 K; spectrum represents average of 8 scans, corrected by subtraction of a buffer baseline spectrum. The number of averaged scans varied from 8-16. The following parameters were used to simulate the 4-coordinate cob(II)alamin spectrum: ^{59}Co (S=1/2, I=7/2); principal g-values, g_x=3.36, g_y=2.49, g_z=1.80; principal hyperfine coupling constants, A_x=1130, A_y=684, A_z=527 MHz; line width=5.9 mT; strain introduced through hyperfine coupling, $\sigma_{A,x}=\sigma_{A,y}$=177, $\sigma_{A,z}$=82.9 MHz.

Crystallography. ATR was crystallized in the presence of ATP from a protein stock (20 mg/ml ATR, 20 mM HEPES pH 7.5, 100 mM NaCl, 1 mM DTT, 2 mM $MgCl_2$) and crystallization reservoir (19% PEG 3350, 0.2 M $MgSO_4$, 10% glycerol 2 mM ATP concentration), as previously reported.[10] Once fully grown, crystals were transferred to fresh drops containing no ATP, and soaked with AdoCbl at a final concentration of 0.5 mM. Crystals were harvested directly from drops and flash-cooled in liquid N_2 at different times after addition of AdoCbl (0.5- 2.5 h). Data were collected at the Advanced Photon Source (APS, Argonne National Laboratory) on GM/CA beamline 23-ID-B. Datasets from the 30 min (d_{min} 2.4 Å) and 1 h (d_{min} 2.85 Å) AdoCbl soak time points were used; longer soak times were deleterious to diffraction. Crystals from both soak times were in the trigonal space group $P3_121$ with one ATR trimer per asymmetric unit. Data were processed using XDS.[11] The structures were solved via molecular replacement using PDB 2IDX[10] as a search model in phaser.[12] Refinement was done with PHENIX[13] and model building in Coot.[14] Ligand restraint files for B_{12} and 5'-deoxyadenosine were from Global Phasing Ltd.[15] The refined models were validated using MolProbity.[16] The structure of ATR from the 30 min AdoCbl soak contained one active site occupied by ATP, one by AdoCbl and PPP_i, and one with AdoCbl only. The presence of PPPi is likely to be the fortuitous outcome of its presence as a contaminant in ATP and its high affinity for ATR in the presence of AdoCbl. The ATR structure from the 1 h soak contained one active site occupied by ATP and two by AdoCbl.

AdoCbl concentration in human fibroblasts. Fibroblasts were obtained from the Mutant Human Cell Strains Repository (McGill University Health Centre) were incubated for 96 h in modified Eagle's minimum essential medium with non-essential amino acids (Wisent Inc, St Lambert CA) supplemented with human serum preincubated with [^{57}Co]-cyanocobalamin (MP Biomedicals, Solon, OH) as a source of human transcobalamin. The final concentration of cyanocobalamin was 25 pg/l. Cells were harvested by trypsinization and cobalamins were extracted with 100% ethanol at 80°C for 20 min. Cobalamins were separated by HPLC as

described.[17] Values are expressed as a percentage of total cell radioactivity. A Student's T test was used to estimate the significance of the difference between control versus patient fibroblast samples ($p<0.05$ was considered to be statistically significant).

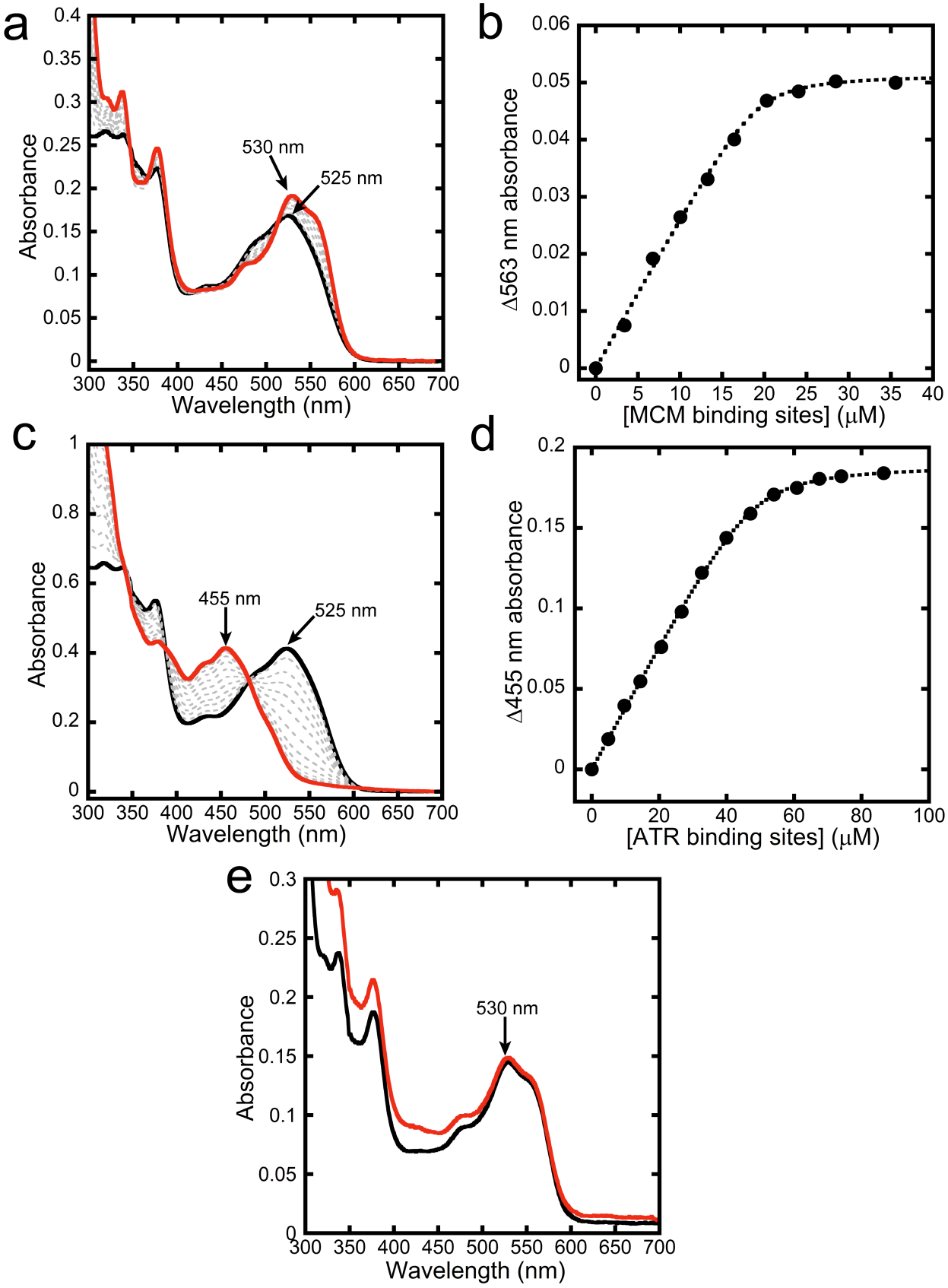
a
Absorbance
Wavelength (nm)
530 nm
525 nm
b
Δ563 nm absorbance
[MCM binding sites] (μM)
c
Absorbance
Wavelength (nm)
455 nm
525 nm
d
Δ455 nm absorbance
[ATR binding sites] (μM)
e
Absorbance
Wavelength (nm)
530 nm

Figure S1. AdoCbl preferentially binds to MCM over ATR. (a) MCM was added to free AdoCbl (20 μM, black line) and the absorption spectra were recorded after each addition of MCM (grey dashed lines). AdoCbl binding to MCM results in a shift in the λ_{max} from 525 nm to 530 nm (red, final spectrum). (b) The change in absorbance at 563 nm versus MCM concentration is plotted and is representative of 4 independent titrations. AdoCbl binds to MCM with an estimated K_d = 0.27±0.11 μM. (c) Addition of ATR to AdoCbl (50 μM) results in a dramatic spectral shift in the λ_{max} from 525 to 455 nm as the cofactor changes from 6-coordinate in solution to 5-coordinate in the ATR active site. (d) The change in absorbance at 455 nm versus ATR concentration is plotted and is representative of 3 independent titrations. AdoCbl binds to ATR with K_d= 0.96 ± 0.31 μM. (e) ATR (133 μM) was added to AdoCbl (20 μM) bound to MCM (20 μM dimer, black line). Insignificant spectral changes were observed even after 20 min (red trace), showing that AdoCbl transfer from MCM to ATR is not detected. Buffer A was used for these titrations as described under Methods.

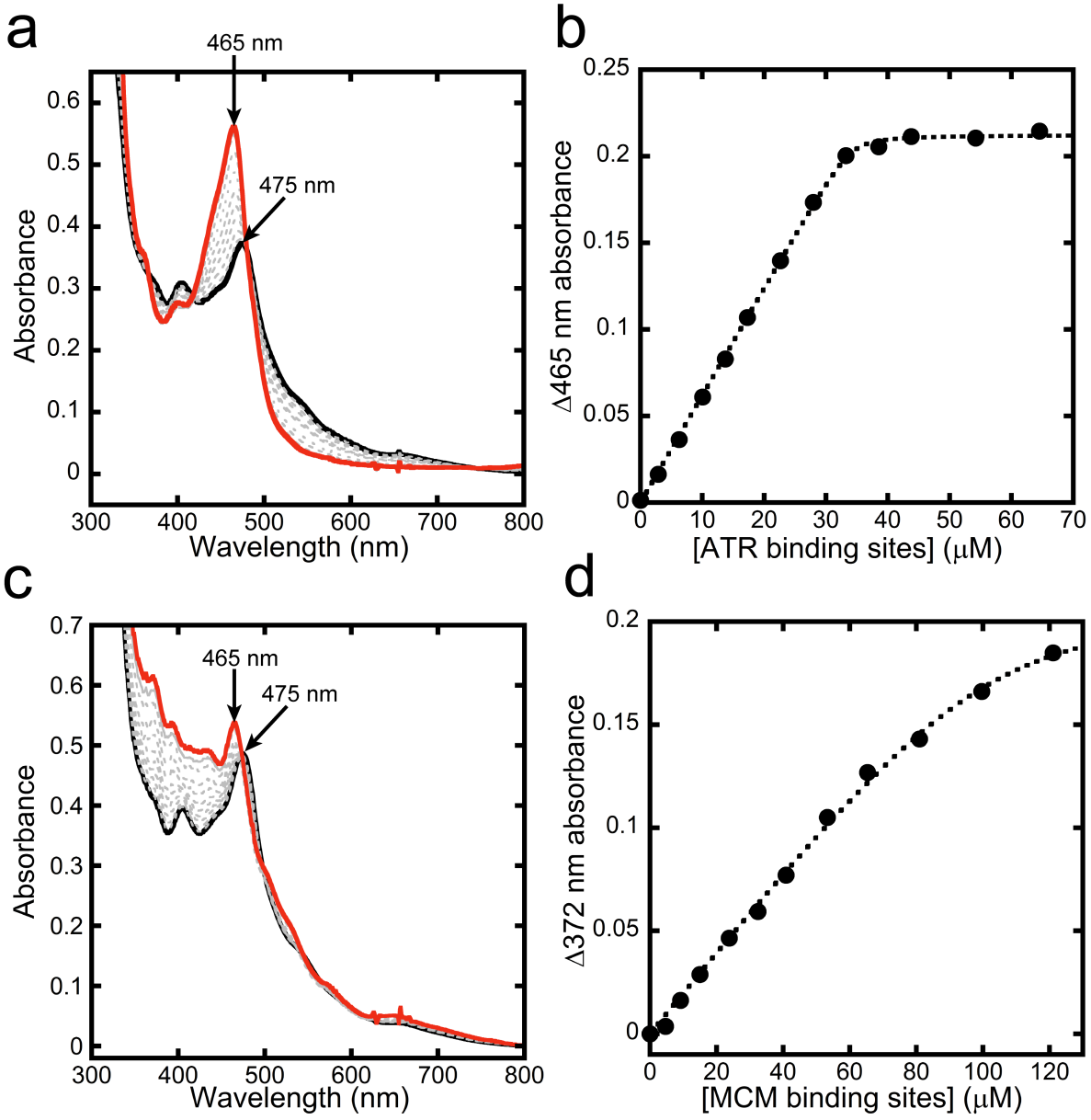

Figure S2. Cob(II)alamin preferentially binds to ATR over MCM. (a) ATR was added to free cob(II)alamin (40 μM, black line) in the presence of 1 mM ATP and the absorption spectra were recorded after each addition of ATR under anaerobic conditions (grey, dashed lines). Cob(II)alamin bound to ATR is 4-coordinate and exhibits a high molar absorptivity at 465 nm (red trace). (b) The change in 465 nm absorbance versus ATR concentration, yields an estimated K_d of 0.08±0.01 μM. (c) MCM was added to cob(II)alamin (50 μM, black line) in the presence of 0.5 mM methylmalonyl-CoA and spectra were recorded after each addition under anaerobic conditions (grey dashed lines). The final spectrum is in red. (d) The change in absorbance at 372 nm versus MCM concentration yields an estimated K_d≥5 μM. The plot is representative of two independent titrations. Buffer A was used for these titrations as described under Methods.

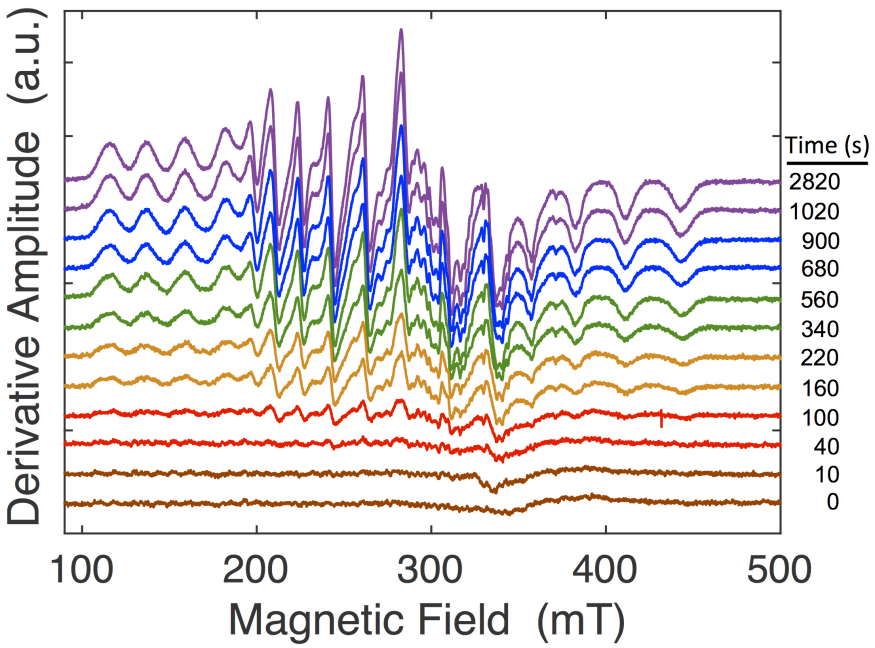

Figure S3. Time-dependent changes in the EPR spectrum of cob(II)alamin triggered by addition of PPPi to ATR•AdoCbl under aerobic conditions. PPP_i (1 mM) was added to 250 μM wild-type ATR (trimer) in 50 mM HEPES buffer, pH 7.5 containing 150 mM KCl, 2 mM $MgCl_2$, 2 mM TCEP and 15% glycerol and 600 μM AdoCbl. Zero-time corresponds to the sample quenched in an isopentane bath (*T*=140 K) immediately after addition of PPP_i. The sample was subsequently thawed, incubated at room temperature for the indicated times, and quenched for spectral acquisition. Microwave frequency, 9.45 GHz; power, 2.0 mW; modulation amplitude, 1.0 mT; modulation frequency, 100 kHz; temperature, 120 K; each spectrum represents the average of 9 scans corrected by subtraction of the buffer baseline spectrum (9 scans); a.u., arbitrary units.

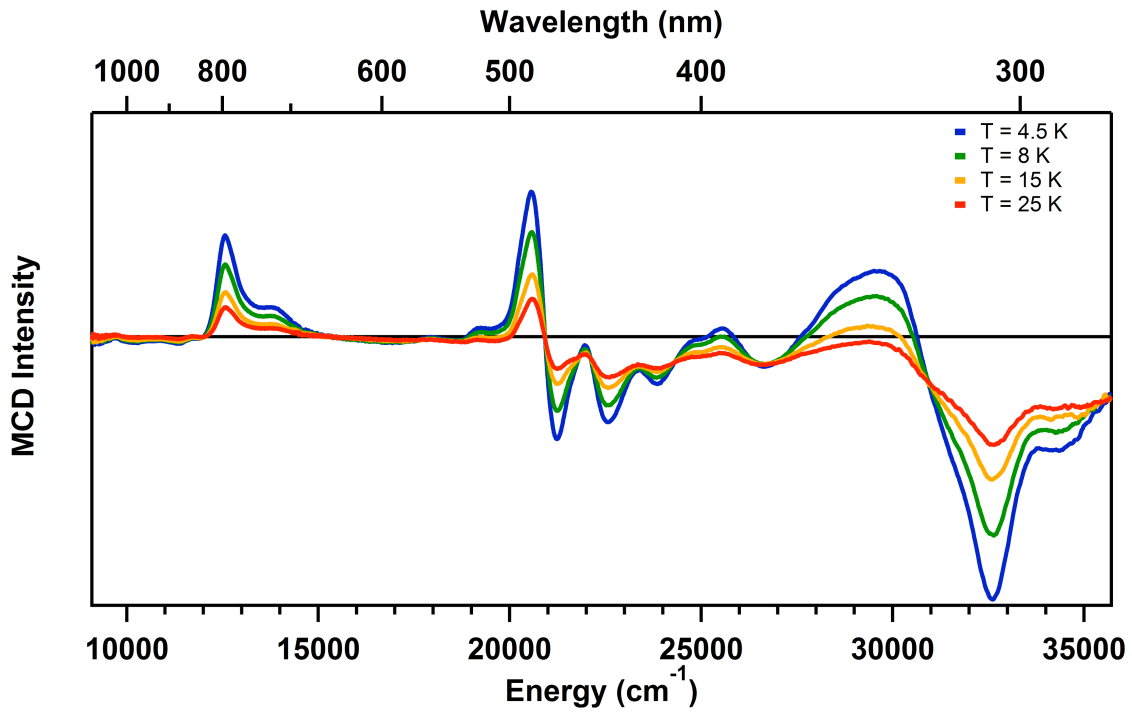

Figure S4. Temperature dependence of the MCD spectrum of ATR-bound cob(II)alamin. MCD spectra at 4.5 K of 4-coordinate cob(II)alamin triggered by addition of PPP_i to wild-type ATR containing AdoCbl under aerobic conditions. Enzyme-bound cob(II)alamin was generated in a reaction mixture containing ATR (99 μM trimer), AdoCbl (197 μM), PPP_i (600 μM) in 50 mM HEPES buffer, pH 7.5 containing 55% glycerol (v/v).

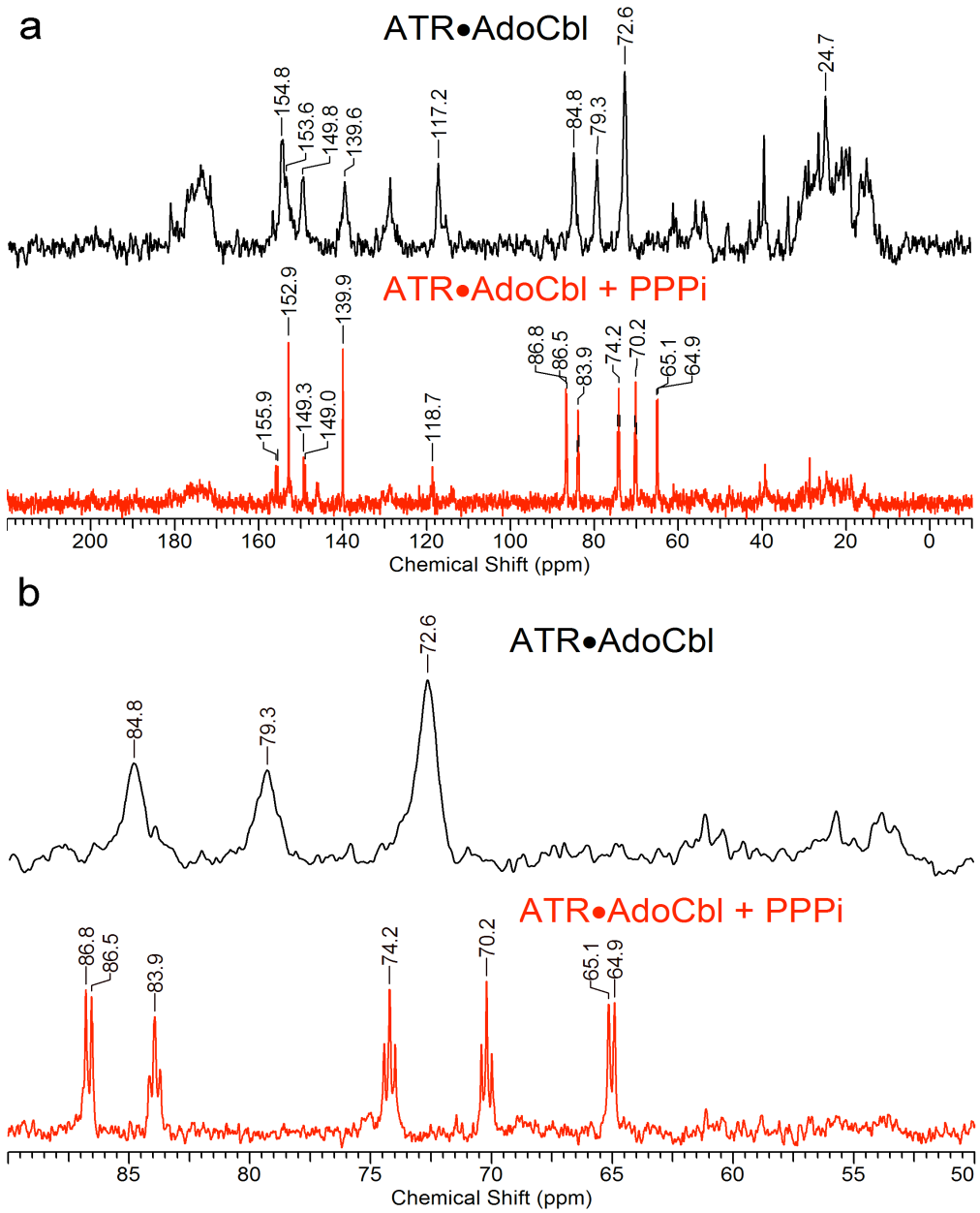

Figure S5. NMR spectrum of the hydroperoxyadenosine product. ^{13}C-NMR spectrum of [U-^{13}C adenosyl]-cobalamin (750 μM) bound to ATR (300 μM, black line) and after incubation with PPP_i (5 mM, red line) at 25°C in 50 mM potassium phosphate buffer pH 7.5, containing 150 mM KCl, 2 mM $MgCl_2$, 2 mM TCEP and 10% D_2O (v/v). (a) Spectra in the -10 to 220 ppm range, and (b) expansion of the 50–90 ppm region to highlight the ^{13}C signals from the ribose moiety are shown. In the red spectrum, the doublet signal at 65.0 ppm corresponds to the 5´ carbon of hydroperoxyadenosine.

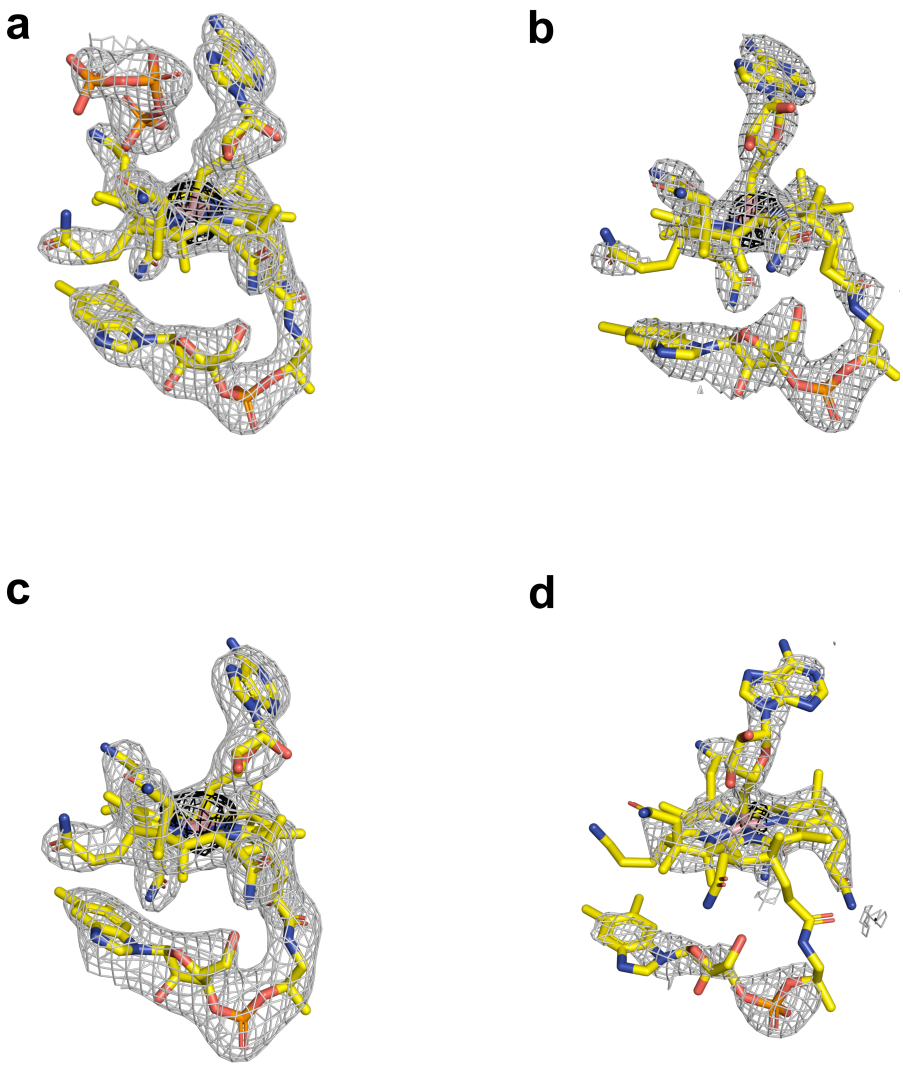

Figure S6. Close-up of ATR active sites showing electron density for AdoCbl and PPPi. Electron density of bound AdoCbl and PPP_i with 2mFo-DFc density shown in grey and the anomalous difference density shown in black. Electron density for the high occupancy AdoCbl and PPPi site (a), 2mFo-DFc contoured at 1.50 σ, anomalous difference density contoured at 5 σ, and the low occupancy AdoCbl site (b), 2mFo-DFc contoured 1.0σ, anomalous difference density contoured to 5σ in the 2.40 Å resolution ATR•AdoCbl•PPPi structure (PDB:6D5X). Electron density for the high occupancy AdoCbl site (c), 2mFo-DFc contoured to 1.50 σ and anomalous difference density contoured to 5σ, and (d) low occupancy AdoCbl site, 2mFo-DFc contoured at 1.0σ and anomalous difference density contoured to 3.5σ in the 2.85 Å resolution ATR•AdoCbl structure (PDB:6D5K).

.

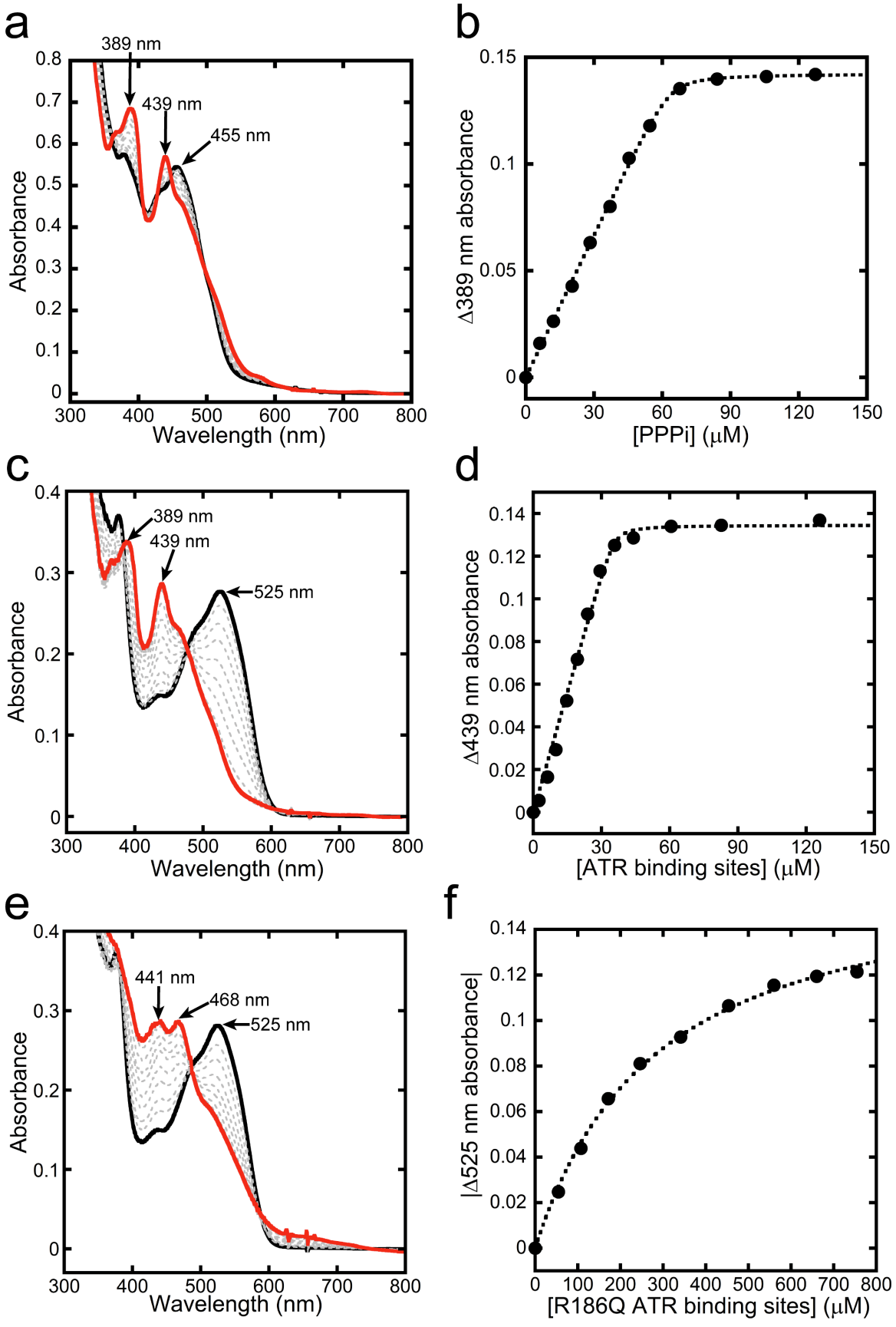
a
389 nm
439 nm
455 nm
Absorbance
Wavelength (nm)
b
Δ389 nm absorbance
[PPPi] (μM)
c
389 nm
439 nm
525 nm
Absorbance
Wavelength (nm)
d
Δ439 nm absorbance
[ATR binding sites] (μM)
e
441 nm
468 nm
525 nm
Absorbance
Wavelength (nm)
f
|Δ525 nm absorbance|
[R186Q ATR binding sites] (μM)

Figure S7. PPPi forms a high affinity ternary complex with AdoCbl•ATR. (a) Titration of PPP_i to AdoCbl•ATR (black trace) under anaerobic conditions results in the formation of intermediate X. In this titration, PPPi was added to ATR (60 μM trimer) loaded with AdoCbl (60 μM). Gray traces represent intermediate spectra during the titration and the red trace is the final spectrum. (b) Representative plot showing the dependence of the absorbance change at 389 nm on PPP_i concentration. PPP_i binds tightly to AdoCbl•ATR (K_d= 0.42 ± 0.08 μM, mean±SD of three independent experiments). (c) Binding of a mixture of AdoCbl (30 μM, black trace) and PPPi (1 mM) to wild-type ATR under anaerobic conditions. Intermediate spectra are show in gray and the final spectrum in red represents intermediate X. (d) Representative plot showing the dependence of the absorbance change at 439 nm on the concentration of ATR. The PPPi•AdoCbl•ATR ternary complex forms with high affinity, with an estimated K_d≤0.2 μM. (e) Binding of a mixture of AdoCbl (30 μM, black trace) and PPPi (5 mM) to R186Q ATR under anaerobic conditions. Intermediate spectra are shown in grey and the final trace of base-on 6-coordinate intermediate X (441 nm) is in red. (f) Representative plot of the change in absorbance at 525 nm versus R186Q ATR shows that the mutant enzyme forms a weak ternary complex with PPPi and AdoCbl (K_d= 240 ± 30 μM, mean±SD of three independent experiments). Buffer A was used for these titrations as described under Methods.

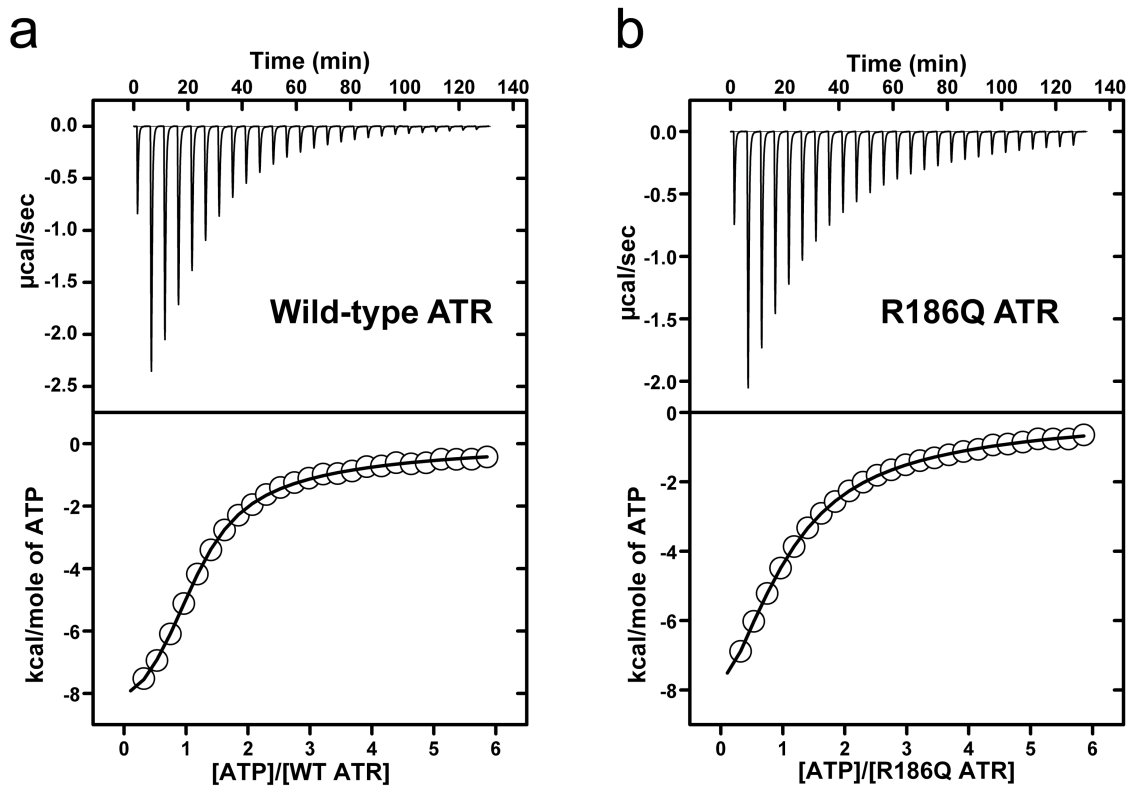

Figure S8. Representative titrations for ATP binding to ATR. ITC was employed to determine the binding affinity of ATP for wild-type (a) and R186Q (b) ATR in Buffer A at 20°C. All titrations were performed at least in triplicate and data were fit to a two-site model per ATR trimer. The K_d values obtained from these titrations are in Table S5.

Table S1

Dissociation constants for ATR and MCM ligands[a]

Enzyme	Ligand	K_d (μM)
MCM	AdoCbl	0.27±0.11
MCM	cob(II)alamin	≥5
wild-type ATR	AdoCbl	0.96 ± 0.31
wild-type ATR•ATP	cob(II)alamin	0.08±0.01
wild-type ATR	AdoCbl +PPPi	≤0.2
wild-type ATR•AdoCbl	PPPi	0.42 ± 0.08
R186Q ATR	AdoCbl	ND[b]
R186Q ATR•ATP	cob(II)alamin	≤0.2
R186Q ATR	AdoCbl +PPPi	240 ± 30
R186Q ATR•AdoCbl	PPPi	ND[b]

[a]Titrations were performed using UV-visible absorption spectroscopy as described in the methods section. The data are the average of 2- (when upper/lower limits for K_d are reported) or 3-4 independent titrations and represent mean±S.D.
[b]N.D. is not detectable

Table S2

Summary of chemical shifts for ATR-bound AdoCbl and 5'-peroxyadenosine generated by sacrificial Co-C bond homolysis.[a]

	^{13}C-AdoCbl•ATR	^{13}C-peroxyadenosine	
	^{13}C Chemical shift [ppm]	^{13}C Chemical shift [ppm] (multiplicity, ^{2}J (^{13}C-^{13}C))	^{1}H Chemical shift [ppm]
1'	84.8	86.7 (*d*, J = 42 Hz)	6.01
2'	72.6	74.2 (*t*, J = 40 Hz)	n.d
3'	72.6	70.2 (*t*, J = 38 Hz)	4.49
4'	79.3	83.9 (*t*, J = 38 Hz)	n.d.
5'	24.7	65.0 (*d*, J = 40 Hz)	4.09/4.17
A2	153.6	152.9 (*s*)	8.14
A4	149.8	149.2 (*d*, J = 63 Hz)	-
A5	117.2	118.7 (*t*, J = 70 Hz)	-
A6	154.8	155.7 (*d*. J = 72 Hz)	-
A8	139.6	139.9 (*s*)	8.41

[a] ^{13}C NMR chemical shifts for ^{13}C-AdoCbl bound to ATR and for ^{13}C-peroxyadenosine generated by addition of PPP_i to ATR•^{13}C-AdoCbl. The ^{13}C-^{13}C coupling constants are only resolved in the presence of PPP_i. ^{1}H chemical shifts were obtained from an HSQC spectrum.

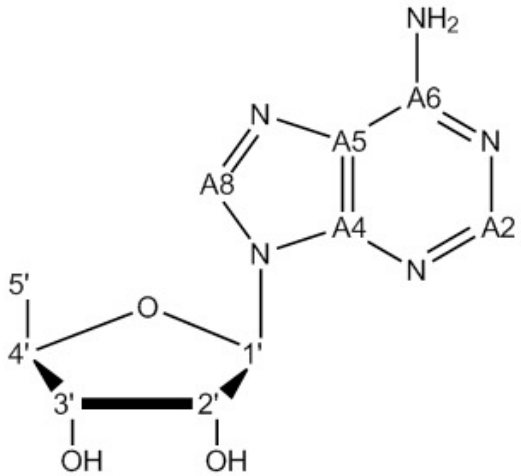

Table S3

Comparison of the predicted ^{1}H and ^{13}C NMR chemical shifts (using the online tool at www.nmrdb.org) and previously reported experimental ^{1}H chemical shifts for 5'-peroxyadenosine.

	Predicted chemical shift of 5' peroxyadenosine		Experimental chemical shift of 5' peroxyadenosine
	^{13}C Chemical shift [ppm]	^{1}H Chemical shift [ppm]	^{1}H Chemical shift [ppm]
1'	88.5	6.29	(5.89) [a]
2'	74.0	4.41	(4.63)
3'	71.4	3.93	(4.15)
4'	82.6	3.76	(4.11)
5'	65.6	4.44	4.06/4.16
A2	153.0	8.49	(8.15)
A4	149.8	-	-
A5	119.8	-	-
A6	156.3	-	-
A8	140.9	7.86	(8.32)

[a]The values in parentheses were not assigned to specific protons.[18]

Table S4

Summary of crystallographic parameters for human ATR.

Diffraction data	**ATR• AdoCbl•PPPi**	**ATR• AdoCbl**
Space group	$P3_121$	$P3_121$
Unit cell a, b, c (Å)	112.7, 112.7, 117.9 (90, 90, 120)	112.3, 112.3, 117.9 (90, 90, 120)
Wavelength (Å)	1.549	1.549
d_{min} (Å)	2.40 (2.49 – 2.40)*	2.85 (2.95 – 2.85)
Observations (#)	338,919 (34,608)	204,544 (20,144)
Unique reflections (#)	34,277 (3,366)	20,510 (2,031)
Mean I/σ_I	16.48 (1.54)	10.78 (0.84)
R_{merge}	0.095 (1.445)	0.189 (2.212)
$CC_{1/2}$	0.99 (0.70)	0.99 (0.43)
CC*	1.00	1.00
Completeness (%)	0.99 (0.99)	0.99 (0.99)
Wilson B ($Å^2$)	59.72	85.11

* Values in parentheses refer to the outermost shell of data.

Table S4 (continued)

Summary of crystallographic parameters for human ATR.

Refinement	ATR• AdoCbl•PPPi	ATR• AdoCbl
Reflections (#)	34,269	20,500
Data Range (Å)	48.79 – 2.40	48.61 – 2.85
R_{work}	0.18	0.19
R_{free}	0.21	0.24
RMSD bonds (Å)	0.006	0.010
RMSD angles (°)	0.83	1.22
Atoms (#)		
Protein	4,037	4,011
Solvent	74	18
Ligand	290	296
Avg B-factors (Å^2)		
Protein	68.9	82.6
Solvent	64.2	75.2
Adocbl1	71.2	76.2
Adocbl2	94.9	136.9
ATP	48.1	61.5
PPPi	101.8	n/a
Ramachandran		
Favored (%)	97.6	98.0
Allowed (%)	2.4	2.0
Outliers (%)	0	0
PDB	6D5X	6D5K

* Values in parentheses refer to the outermost shell of data.

Table S5

Binding affinities for ATP to wild-type and R186Q ATR.[a]

Enzyme	K_{d1} (μM)	K_{d2} (μM)	ΔG_1 (kcal/mol)	ΔG_2 (kcal/mol)	ΔH_1 (kcal/mol)	ΔH_2 (kcal/mol)	$-T\Delta S_1$ (kcal/mol)	$-T\Delta S_1$ (kcal/mol)
ATR	6.3±0.2	134±5	–7.0±0.1	–5.2±0.1	–10.2±1.3	–5.8±2.4	3.2±1.3	0.6±0.2
R186Q ATR	22.1± 0.7	296±21	–6.3±0.1	–4.7±0.1	–8.6±0.9	–15.9±1.1	2.3±0.9	11±1

[a]The ITC titration data are shown in Figure S8. The data are the average of 3 independent titrations and represent the mean±SD.

References

1. Froese, D. S.; Kochan, G.; Muniz, J. R. C.; Wu, X.; Gileadi, C.; Ugochukwu, E.; Krysztofinska, E.; Gravel, R. A.; Oppermann, U.; Yue, W. W., Structures of the Human GTPase MMAA and Vitamin B12-dependent Methylmalonyl-CoA Mutase and Insight into Their Complex Formation. *J Biol Chem* **2010,** *285* (49), 38204-38213.

2. Kuzmič, P., Program DYNAFIT for the Analysis of Enzyme Kinetic Data: Application to HIV Proteinase. *Anal Biochem* **1996,** *237* (2), 260-273.

3. Pratt, J. M., *Inorganic Chemistry of Vitamin B_{12}*. Academic Press: London, 1972.

4. Li, Z.; Kitanishi, K.; Twahir, U. T.; Cracan, V.; Chapman, D.; Warncke, K.; Banerjee, R., Cofactor Editing by the G-protein Metallochaperone Domain Regulates the Radical B12 Enzyme IcmF. *J Biol Chem* **2017,** *292* (10), 3977-3987.

5. Waddington, M. D.; Finke, R. G., Neopentylcobalamin (neopentylB12) cobalt-carbon bond thermolysis products, kinetics, activation parameters, and bond dissociation energy: a chemical model exhibiting 106 of the 1012 enzymic activation of coenzyme B12's cobalt-carbon bond. *J Am Chem Soc* **1993,** *115* (11), 4629-4640.

6. Schrauzer, G. N.; Grate, J. H., Sterically induced, spontaneous cobalt-carbon bond homolysis and .beta.-elimination reactions of primary and secondary organocobalamins. *J Am Chem Soc* **1981,** *103* (3), 541-546.

7. Harris, R. K.; Becker, E. D.; Cabral de Menezes, S. M.; Goodfellow, R.; Granger, P., NMR nomenclature: nuclear spin properties and conventions for chemical shifts. IUPAC Recommendations 2001. International Union of Pure and Applied Chemistry. Physical Chemistry Division. Commission on Molecular Structure and Spectroscopy. *Magnetic Resonance in Chemistry* **2002,** *40* (7), 489-505.

8. Stich, T. A.; Yamanishi, M.; Banerjee, R.; Brunold, T. C., Spectroscopic evidence for the formation of a four-coordinate Co^{2+} cobalamin species upon binding to the human ATP:cobalamin adenosyltransferase. *J Am Chem Soc* **2005,** *127* (21), 7660-1.

9. Wang, M.; Zhu, C.; Kohne, M.; Warncke, K., Resolution and Characterization of Chemical Steps in Enzyme Catalytic Sequences by Using Low-Temperature and Time-Resolved, Full-Spectrum EPR Spectroscopy in Fluid Cryosolvent and Frozen Solution Systems. *Methods Enzymol* **2015,** *563*, 59-94.

10. Schubert, H. L.; Hill, C. P., Structure of ATP-Bound Human ATP:Cobalamin Adenosyltransferase. *Biochemistry* **2006,** *45* (51), 15188-96.

11. Kabsch, W., XDS. *Acta Crystallogr D* **2010,** *66* (Pt 2), 125-32.

12. McCoy, A. J.; Grosse-Kunstleve, R. W.; Adams, P. D.; Winn, M. D.; Storoni, L. C.; Read, R. J., Phaser crystallographic software. *J Appl Crystallogr* **2007,** *40* (Pt 4), 658-674.

13. Adams, P. D.; Afonine, P. V.; Bunkoczi, G.; Chen, V. B.; Davis, I. W.; Echols, N.; Headd, J. J.; Hung, L. W.; Kapral, G. J.; Grosse-Kunstleve, R. W.; McCoy, A. J.; Moriarty, N. W.; Oeffner, R.; Read, R. J.; Richardson, D. C.; Richardson, J. S.; Terwilliger, T. C.; Zwart, P. H., PHENIX: a comprehensive Python-based system for macromolecular structure solution. *Acta Crystallogr D Biol Crystallogr* **2010,** *66* (Pt 2), 213-21.

14. Emsley, P.; Lohkamp, B.; Scott, W. G.; Cowtan, K., Features and development of Coot. *Acta Crystallogr D Biol Crystallogr* **2010,** *66* (Pt 4), 486-501.

15. Smart, O. S.; Womack, T. O.; Sharff, A.; Flensburg, C.; Keller, P.; Paciorek, W.; Vonrhein, C.; Bricogne, G., Global Phasing Ltd: Cambridge, U.K., 2011; p grade v.1.2.13.

16. Chen, V. B.; Arendall, W. B., 3rd; Headd, J. J.; Keedy, D. A.; Immormino, R. M.; Kapral, G. J.; Murray, L. W.; Richardson, J. S.; Richardson, D. C., MolProbity: all-atom structure validation for macromolecular crystallography. *Acta Crystallogr D Biol Crystallogr* **2010,** *66* (Pt 1), 12-21.

17. Jacobsen, D. W.; Green, R.; Quadros, E. V.; Montejano, Y. D., Rapid analysis of cobalamin coenzymes and related corrinoid analogs by high-performance liquid chromatography. *Anal Biochem* **1982,** *120* (2), 394-403.

18. Schwartz, P. A.; Frey, P. A., 5‘-Peroxyadenosine and 5‘-Peroxyadenosylcobalamin as Intermediates in the Aerobic Photolysis of Adenosylcobalamin. *Biochemistry* **2007,** *46* (24), 7284-7292.